XLIII CILAMCE
21-25, November, 2022
FOZ DO IGUAÇU - PR - BRAZIL

Phase-field model for pressurized fractures simulation

Eduarda M. Ferreira[1], Roque L. S. Pitangueira [1], Lapo Gori[1]

[1]*Structural Engineering Department, Federal University of Minas Gerais*
Av. Antonio Carlos, 6627, Pampulha, Belo Horizonte, 31270-901, Minas Gerais, Brazil
eduardaferreira@ufmg.br, roque@dees.ufmg.br, lapo@dees.ufmg.br

Abstract. The present work investigates the numerical simulation of pressurized fracture, using the phase-field strategy, and its implementation. A simplified approach to hydraulic fracture with phase-field already available in the literature, is implemented in the open-source software INSANE (INteractive Structural ANalysis Environment) developed at the Structural Engineering Department of the Federal University of Minas Gerais, taking advantage of its object-oriented structure. Within this simplified model, inertial and leak-off effects are neglected, the reservoir is considered impermeable and the fluid incompressible, leading to a fracture system where the fluid pressure is constant. The pressure load is applied directly on the fracture surface influencing its behavior. Numerical simulations performed with the finite element method are presented, aiming to illustrate the model as well as to evaluate the initial results found with regard to the behavior of the crack subjected to pressure load.

Keywords: Phase-field model, Pressurized fractures, INSANE software

1 Introduction

Fracture is an important failure mechanism that has been intensively studied in recent years in the field of structural engineering as a way of investigating its behavior and possible consequences for the material and structural behaviors. A particular type of fracture is the hydraulic fracture or, for simpler models, the pressurized fracture. The problem of pressurized fracture can occur in several situations, such as in the case of dams, submerged structures and fluid reservoirs. The study of hydraulic fracturing is also fundamental for various applications as geophysical processes, geotechnical applications, mining operations and geothermal reservoirs ([1]).

Recently, several models and numerical techniques have been proposed to simulate pressurized fracture and crack propagation in elastic and porous media. Wheeler et al. [2] points out that the work of Bourdin et al. [3] was the first to use phase-field model to pressurized cracks. The benefits of the phase-field model are many, such as the use of a fixed mesh during the entire analysis and the power to detect the appearance, propagation, nucleation and bifurcation of cracks without any additional techniques. Furthermore, it is possible to work with an indefinite number of pre-existing or propagating cracks without limiting their propagation directions.

In this first application, Bourdin et al. [3] propose an extension of the variational approach to fracture of Francfort and Marigo [4] to account for pressure forces along the crack surface. It is a simplified model where inertial and leak-off effects are neglected, the reservoir is considered impermeable and the fluid incompressible, leading to a fracture system where the fluid pressure is constant.

Other authors also employed the variational approach in the study of hydraulic fractures, as is the case of Yoshioka and Bourdin [5] and Singh et al. [6]. Yoshioka and Bourdin [5] presents a coupled model of the hydraulic fracture problem to an external reservoir simulator. In this model, in addition to considering the in-situ stresses that are required in hydraulic applications, poro-elasticity is also considered. Singh et al. [6] also makes use of the energy minimization principles but with the proposal of a hybrid model where the phase-field would affect only the fluid domain without affecting the solid domain. This domain separation is done by adopting a phase-field threshold value that would define the loading boundary, which is exactly the boundary between the domains.

In the present work, the pressurized fracture model described by Bourdin et al. [3] was adopted, considering a constant pressure load. The computational implementation of this model was carried out in the object-oriented programming environment of the INSANE software.

In the next section, a summary of the variational approach to pressurized fractures presented by Bourdin et al. [3] will be exhibit and then the application of this model in two numerical examples with some initial conclusions.

2 The variational approach to pressurized fractures

The variational approach to fracture consists on the minimization of the total energy functional for any kinematically admissible displacement field u and any crack configuration Γ as long as it is fulfilled the irreversible nature of the fracture process. A pressure-loaded fracture problem can be depicted by the schematic representation in Fig. 1.

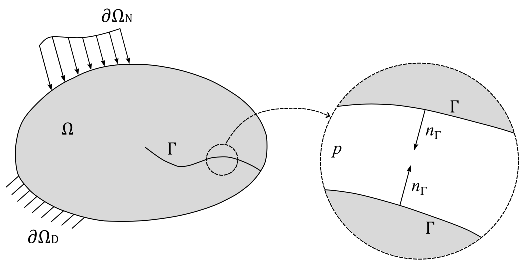

Figure 1. Representation of the pressure-loaded fracture problem

In Fig. 1, Ω is the problem domain with external boundary $\partial\Omega$. The external boundary is decomposed in a part $\partial\Omega_D$ on which Dirichlet conditions are imposed and another part $\partial\Omega_N$ on which Neumann conditions are imposed. Γ represents the crack set, p is the pressure load along the crack surface and n_Γ are the normal vectors to the crack surface.

The energy functional for a problem that does not involve the presence of pressure load in the crack region can be expressed by eq. (1):

$$E(u,\Gamma) = \int_\Omega \psi_0(\varepsilon(u))\, d\Omega - \int_\Omega b \cdot u \, d\Omega - \int_{\partial\Omega_N} \tau \cdot u \, dS + G_c \mathcal{H}^{N-1}(\Gamma), \tag{1}$$

where ψ_0 is the elastic strain energy density associated with the strain field $\varepsilon(u)$, τ and b denote surface and body forces applied to Ω, and $\mathcal{H}^{N-1}(\Gamma)$ represents the measure of Γ which can be its length or area, depending on the dimension of the problem. G_c is the critical energy rate and, according to the known Griffith criterion, the crack starts growing when elastic energy restitution rate G, caused by an infinitesimal increase on the crack surface, matches G_c.

To overcome the challenges of tracking the crack network explicitly, Bourdin et al. [3] uses the resource to work with the regularized problem using the phase-field approach. In that, the crack location is represented by a continuous field variable ϕ that assumes values from zero to one, being one in the crack and zero far from it, in addition to represents a smooth transition between the cracked and intact regions. The regularization parameter l_0 is called length scale parameter in phase-field models and is related to the size of the degraded region. The energy expression for the regularized problem is given by eq. (2):

$$E^r(u,\phi) = \int_\Omega \psi(\varepsilon(u),\phi)\, d\Omega - \int_\Omega b \cdot u \, d\Omega - \int_{\partial\Omega_N} \tau \cdot u \, dS + \int_\Omega G_c \gamma(\phi, \nabla\phi)\, d\Omega, \tag{2}$$

where ψ is the strain energy and γ is crack surface density function. When $l_0 \to 0$ the model approximates that of a sharp fissure and $E^r \to E$.

In order to account for pressure forces along the crack surfaces it is necessary to know the work of that pressure forces W_p. Being p the constant pressure acting along each side of the cracks, it can be written:

$$W_p = \int_\Gamma p\, [[u]] \cdot n_\Gamma \, dS, \tag{3}$$

where $[[u]] = (u^+ - u^-)$ and n_Γ is the fracture outward-pointing normal vector. Equation (3) can also be approximate to the regularized problem and the total energy functional to pressurized fractures becomes:

$$E_t(u,\Gamma) = \int_\Omega \psi(\varepsilon(u),\phi)\, d\Omega - \int_\Omega b\cdot u\, d\Omega - \int_{\partial\Omega_N} \tau\cdot u\, dS + \int_\Omega G_c\gamma(\phi,\nabla\phi)\, d\Omega + \int_\Omega p\, u\cdot\nabla\phi\, d\Omega. \quad (4)$$

The total energy functional minimization given by eq. (4) is achieved by an alternate minimization with respect to the *u* and ϕ, until global convergence. For that, first it is computed *u* by minimizing eq. (4) with respect to *u*. The first variation of the energy functional with respect to *u* is given by:

$$\delta E_t(u,\phi,p,\delta u) = -\int_\Omega (\nabla\sigma + b)\cdot\delta u\, d\Omega + \int_{\partial\Omega_N} (\sigma\cdot n - \tau)\cdot\delta u\, dS + \int_\Omega p(\nabla\phi\cdot\delta u) d\Omega. \quad (5)$$

The last integral of eq. (5) represents the work exerted by the pressure load in the fracture surface which is accounted for by a volumetric body force in a neighborhood of the cracks.

Second it is computed ϕ by minimizing eq. (4) with respect to ϕ. The first variation of the energy functional with respect to ϕ is given by:

$$\delta E_t(u,\phi,p,\delta\phi) = \int_\Omega \left[\frac{\partial\psi}{\partial\phi} + G_c\left(\frac{\partial\gamma}{\partial\phi} - \nabla\cdot\frac{\partial\gamma}{\partial\nabla\phi}\right)\right]\delta\phi d\Omega + \int_\Omega G_c\left(\frac{\partial\gamma}{\partial\nabla\phi}\cdot n\right)\delta\phi\, d\Omega + \int_\Omega p(u\cdot\nabla\delta\phi) d\Omega. \quad (6)$$

3 Implementation

This work presents some initial results that were obtained expanding the already existing phase-field model for frature in the software INSANE (INteractive Structural ANalysis Environment) to account for pressure forces along the crack surfaces. The INSANE is an open-source software developed at the Structural Engineering Department of the Federal University of Minas Gerais (UFMG) based on the Object-Oriented Programming. More details about the phase-field model, its finite element discretization and computational implementation in INSANE software can be seen in the works of Leão et al. [7], Leão et al. [8], Bayão et al. [9] and Fortes et al. [10].

Additions were made to the already implemented phase-field model to account for the effect of pressure loading in the crack region. Before each step, the pressure force is applied, according to the formulation, to the elements affected by a phase-field gradient and only then the displacement field is determined. After that, the convergence of the phase-field variable is performed. The governing equation from residual phase-field was also modified by a term containing the pressure load, originated from the last integral of the equation eq. (6).

In the simulations that will be presented a bound-constrained based staggered solver was adopted, which guarantees the condition of irreversibility of the crack with an additional condition imposed in the calculation of the nodal phase-field.

4 Numerical examples

4.1 Tension test

The first example represents a simple problem involving tension as seen in Fig. 2a. A Q4 mesh with $h = 0.05$ mm was adopted as shown in Fig. 2b. This problem used the constitutive model presented by Miehe et al. [11] and the following parameters: Young's modulus $E = 25850$ N/mm², Poisson's ration $\nu = 0.18$, shear modulus $G = 10953.39$ N/mm², fracture energy $G_c = 0.065$ N/mm, length scale $l_0 = 0.1$ mm. For crack geometry function was used $\alpha = \phi^2$, and for energy degradation function was used $g = (1-\phi)^2$, both the quadratic functions proposed by Bourdin et al. [12].

The problem was defined in plain stress. The complete simulation had 200 steps, with a tolerance for phase-field, displacements and global convergences equals to 10^{-4}. A displacement strategy control was used considering increments of 10^{-4} mm at all nodes of the right side of the mesh. The nodes situated along the predefined crack had a $\phi = 1$ constraint imposed since the beginning of the analysis.

Figure 3 shows phase-field contour plots for the problem considering pressure load $p = 0$ N/mm² and $p = 1$ N/mm². The analysis for $p = 1$ N/mm² only achieve convergence until step 26, requiring further investigation of

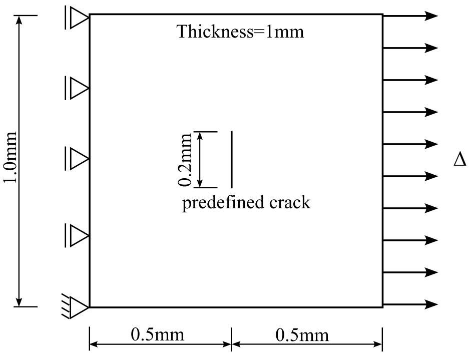

(a) Problem setting

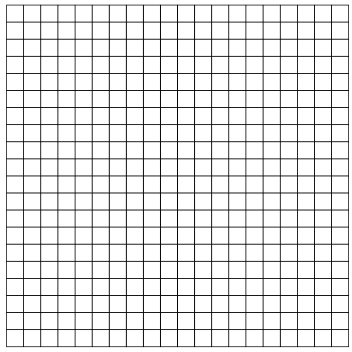

(b) Q4 mesh

Figure 2. Tension test

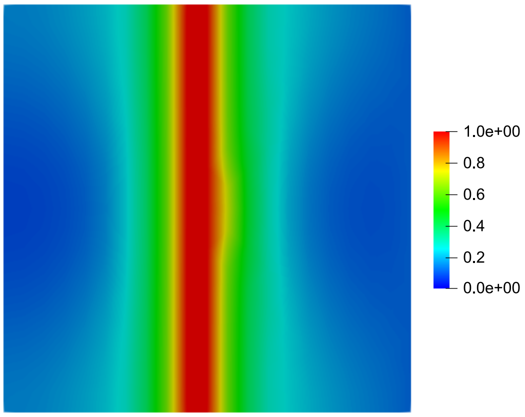

(a) $p = 0N/mm^2$ (step 200)

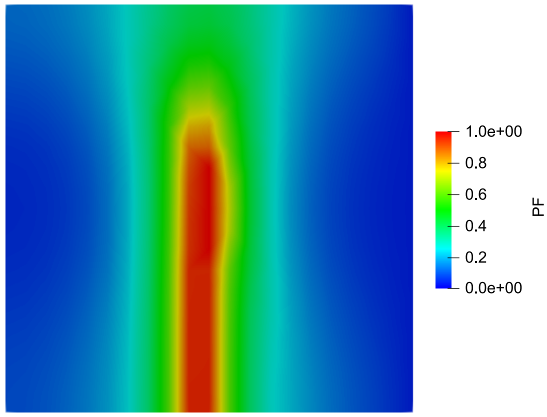

(b) $p = 1N/mm^2$ (step 26)

Figure 3. Phase-field contour plots

the reason for the lack of convergence from this step forward. The phase-field profile for $p = 0.1$ N/mm² and $p = 0.3$ N/mm² are too similar to the one found for $p = 0$ N/mm² and therefore were omitted.

The obtained results for load-displacement curves for each pressure load case studied are shown in Fig. 4. Through the graph it is possible to see that the final load factor gradually decreases with the increase of the pressure load value inserted in the model. The result found is consistent since the material properties and controlled displacement were maintained and the structure is being subjected to a greater load with increasing pressure load.

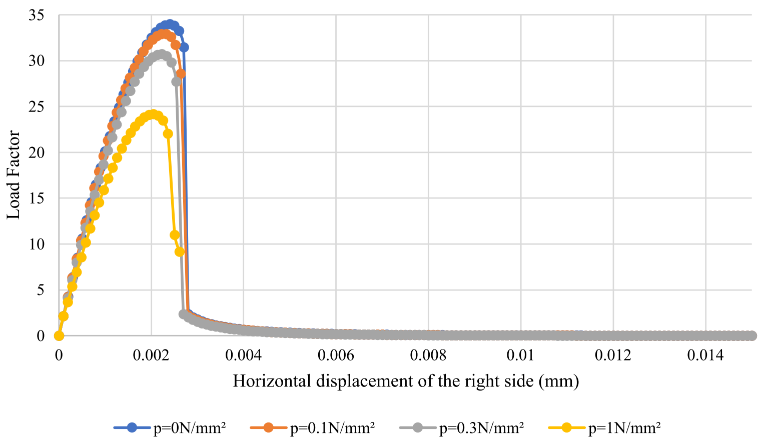

Figure 4. Load-displacement curves of the right side for each pressure load value

4.2 Three point bending beam

This second example is the three point bending beam inspired by the model studied by Petersson [13]. The problem setting can be seen in Fig. 5. The mesh composed of quadrilateral elements with four nodes is presented in Fig. 5. The nodal mean distance is 10 mm in the refined region and 50 mm in the unrefined region.

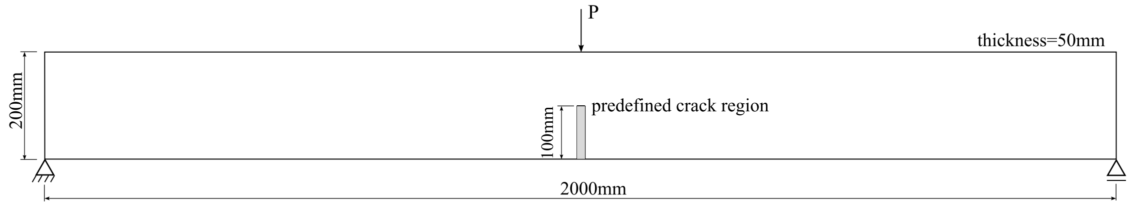

Figure 5. Problem setting for the three point bending beam

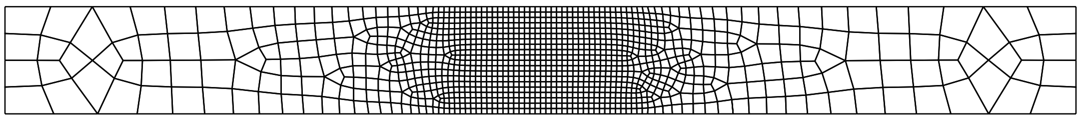

Figure 6. Mesh for the three point bending beam

In order to compare two different constitutive models and verify their behavior when the structure is subjected to a pressure load in the crack region, computer simulations were carried out with the constitutive model of Miehe et al. [11] and of Wu [14]. In both analyzes, the quadratic crack geometry function proposed by Wu [14], given by $\alpha(\phi) = \xi\phi + (1-\xi)\phi^2$, was used, with $\xi = 2$, and for energy degradation function was also used the one proposed by Wu [14] with Cornelissens's law for concrete.

The problem was defined in plain stress, with a reference load of $1N$. The analysis had 800 steps, with a global and local tolerance of 10^{-4}. A displacement strategy control was used in the load application node with increments of -0.004 mm for its vertical displacement. For both constitutive models were employed the following material proprieties: $E = 30000$ N/mm², $\nu = 0.2$, $l_0 = 20$mm, $f_t = 3.3$ N/mm², $G_c = 0.124$ N/mm. The pressure loading is taken as $p = 1$ N/mm². It should be noted that, for this example, the simulations with and without pressure loading completed the 800 steps of the analysis.

The geometric discontinuity present in the structure from Petersson [13] was replaced by a predefined crack obtained in the present model by restricting the phase-field variable ϕ to a unit value in that region. This can be seen in the Fig. 7a that shows the initial phase-field distribution for step 0 in all analysis. The final phase-field profile to the problem without pressure load and constitutive model of Miehe et al. [11] is shown in Fig. 7b, which is very similar to what was obtained with the constitutive model of Wu [14], which for that reason was omitted. However, when a pressure load p is considered in the crack regions according to the model previously presented, some differences, albeit small, are noted in the phase-field distribution along the beam. These differences can be seen in Fig. 7c and Fig. 7d.

5 Conclusions

This paper presented the initial results obtained with the application of the model proposed by Bourdin et al. [3] for problems of pressurized fractures with constant pressure load and impermeable surfaces.

In a first example of tension test, the effect of the variation of the pressure load was investigated. As the case with the highest pressure load had its convergence interrupted before the analysis was completed, it was not possible to carry out a complete comparison of the phase-field profiles. However, the equilibrium trajectories showed a behavior consistent with the expected that the load factor would decrease with increasing pressure, since the control displacement was maintained.

In the second example it was possible to observe that the pressure load causes a faster propagation of the crack, which also presents a more smeared behavior. While in the model without the pressure load the crack only

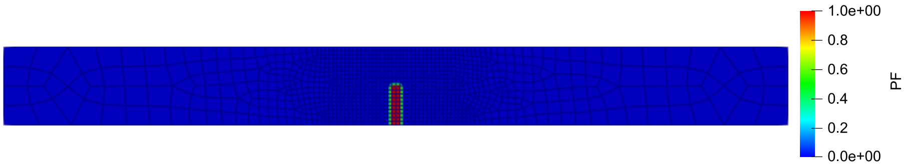

(a) Initial step configuration

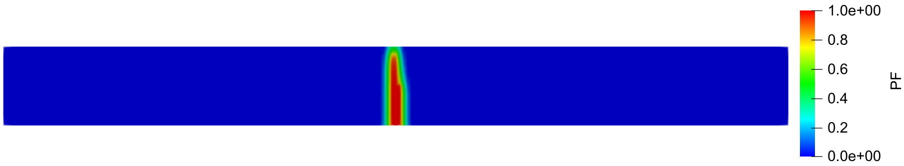

(b) Without pressure load (constitutive model of Miehe et al. [11])

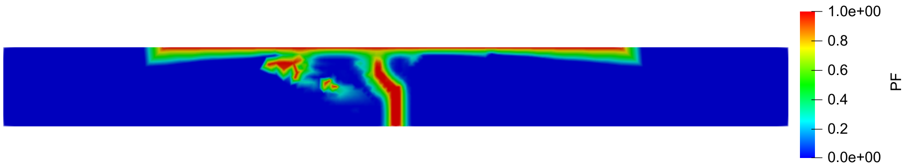

(c) With pressure load (constitutive model of Wu [14]))

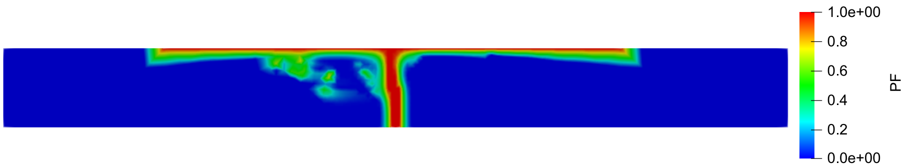

(d) With pressure load (constitutive model of Miehe et al. [11])

Figure 7. Phase-field profiles

propagates from its initial configuration towards the load application point, in the pressurized fracture model it was observed that the damaged region spread to a large part of the top of the beam.

In this second example, a comparison was also made between the phase-field profiles obtained with the application of two different constitutive models. In this case, although differences were identified, the overall behavior seems to have been maintained. As only two constitutive models were analyzed in a single example, it was not possible to draw further conclusions regarding their influences on the behavior of the pressurized crack.

Finally, it can be said that the model presentend by Bourdin et al. [3] was able to represent the behavior of simple problems where the crack region suffers an external stimulus from a pressure load.

Acknowledgements. The authors gratefully acknowledge the support from the Brazilian research agencies CAPES (*Coordenação de Aperfeiçoamento de Pessoal de Nível Superior*), FAPEMIG (*Fundação de Amparo à Pesquisa do Estado de Minas Gerais*; Grant PPM-00747-18) and CNPq (Conselho Nacional de Desenvolvimento Científico e Tecnológico; Grant 316240/2021-4).

Authorship statement. The authors hereby confirm that they are the sole liable persons responsible for the authorship of this work, and that all material that has been herein included as part of the present paper is either the property (and authorship) of the authors, or has the permission of the owners to be included here.

References

[1] C. Chukwudozie, B. Bourdin, and K. Yoshioka. A variational phase-field model for hydraulic fracturing in porous media. *Computer methods in applied mechanics and engineering*, vol. 347, pp. 957–982, 2019.

[2] M. F. Wheeler, T. Wick, and W. Wollner. An augmented-lagrangian method for the phase-field approach for pressurized fractures. *Computer methods in applied mechanics and engineering*, vol. 271, pp. 69–85, 2014.

[3] B. Bourdin, C. Chukwudozie, and K. Yoshioka. A variational approach to the numerical simulation of hy-

draulic fracturing. *Proceedings of the 2012 SPE Annual Technical Conference and Exhibition*, vol. SPE 146951, 2012.

[4] G. A. Francfort and J. J. Marigo. Revisiting brittle fracture as an energy minimization problem. *Journal of the Mechanics and Physics of Solids*, vol. 46, n. 8, pp. 1319–1342, 1998.

[5] K. Yoshioka and B. Bourdin. A variational hydraulic fracturing model coupled to a reservoir simulator. *International Journal of Rock Mechanics Mining Sciences*, vol. 88, pp. 137–150, 2016.

[6] N. Singh, C. V. Verhoosel, and van E. H. Brummelen. Finite element simulation of pressure-loaded phase-field fractures. *Meccanica*, vol. 53, pp. 1513–1545, 2017.

[7] H. M. Leão, R. L. S. Pitangueira, and L. Gori. Phase-field modelling of diffuse fracture with fem. *XLI Ibero-Latin American Congress on Computational Methods in Engineering (CILAMCE)*, 2020.

[8] H. M. Leão, M. M. Fortes, R. G. Bayão, L. Gori, and R. L. S. Pitangueira. Oop implementation of phase-field models. *XLII Ibero-Latin American Congress on Computational Methods in Engineering (CILAMCE)*, 2021.

[9] R. G. Bayão, H. M. Leão, M. M. Fortes, L. Gori, and R. L. S. Pitangueira. Implementation of a bound-constrained solver in phase-field modelling of fracture. *XLII Ibero-Latin American Congress on Computational Methods in Engineering (CILAMCE)*, 2021.

[10] M. M. Fortes, H. M. Leão, R. G. Bayão, L. Gori, and R. L. S. Pitangueira. A bound-constrained solver for phase-field modelling of diffuse fracture. *XLII Ibero-Latin American Congress on Computational Methods in Engineering (CILAMCE)*, 2021.

[11] C. Miehe, F. Welschinger, and M. Hofacker. Thermodynamically consistent phase-field models of fracture: Variational principles and multi-field fe implementations. *International Journal for Numerical Methods in Engineering*, vol. 83, pp. 1273–1311, 2010.

[12] B. Bourdin, G. A. Francfort, and J. J. Marigo. Numerical experiments in revisited brittle fracture. *Journal of the Mechanics and Physics of Solids*, vol. 48, pp. 797–826, 2000.

[13] P.-E. Petersson. Crack growth and development of fracture zones in plain concrete and similar materials. *JTech. Rep. TVBM-1006, Division of Building Materials, Lund Institute of Technology, Lund, Sweden*, 1981.

[14] J. Wu. A unified phase-field theory for the mechanics of damage and quasi-brittle failure. *Journal of the Mechanics and Physics of Solids*, vol. 103, pp. 72–99, 2017.